Fermilab-Pub-10/203-E

Search for flavor changing neutral currents via quark-gluon couplings in single top quark production using 2.3 fb^{-1} of $p\bar{p}$ collisions

V.M. Abazov,[35] B. Abbott,[73] M. Abolins,[62] B.S. Acharya,[29] M. Adams,[48] T. Adams,[46] G.D. Alexeev,[35] G. Alkhazov,[39] A. Alton[a],[61] G. Alverson,[60] G.A. Alves,[2] L.S. Ancu,[34] M. Aoki,[47] Y. Arnoud,[14] M. Arov,[57] A. Askew,[46] B. Åsman,[40] O. Atramentov,[65] C. Avila,[8] J. BackusMayes,[80] F. Badaud,[13] L. Bagby,[47] B. Baldin,[47] D.V. Bandurin,[46] S. Banerjee,[29] E. Barberis,[60] A.-F. Barfuss,[15] P. Baringer,[55] J. Barreto,[2] J.F. Bartlett,[47] U. Bassler,[18] S. Beale,[6] A. Bean,[55] M. Begalli,[3] M. Begel,[71] C. Belanger-Champagne,[40] L. Bellantoni,[47] J.A. Benitez,[62] S.B. Beri,[27] G. Bernardi,[17] R. Bernhard,[22] I. Bertram,[41] M. Besançon,[18] R. Beuselinck,[42] V.A. Bezzubov,[38] P.C. Bhat,[47] V. Bhatnagar,[27] G. Blazey,[49] S. Blessing,[46] K. Bloom,[64] A. Boehnlein,[47] D. Boline,[70] T.A. Bolton,[56] E.E. Boos,[37] G. Borissov,[41] T. Bose,[59] A. Brandt,[76] O. Brandt,[23] R. Brock,[62] G. Brooijmans,[68] A. Bross,[47] D. Brown,[19] X.B. Bu,[7] D. Buchholz,[50] M. Buehler,[79] V. Buescher,[24] V. Bunichev,[37] S. Burdin[b],[41] T.H. Burnett,[80] C.P. Buszello,[42] P. Calfayan,[25] B. Calpas,[15] S. Calvet,[16] E. Camacho-Pérez,[32] J. Cammin,[69] M.A. Carrasco-Lizarraga,[32] E. Carrera,[46] B.C.K. Casey,[47] H. Castilla-Valdez,[32] S. Chakrabarti,[70] D. Chakraborty,[49] K.M. Chan,[53] A. Chandra,[78] G. Chen,[55] S. Chevalier-Théry,[18] D.K. Cho,[75] S.W. Cho,[31] S. Choi,[31] B. Choudhary,[28] T. Christoudias,[42] S. Cihangir,[47] D. Claes,[64] J. Clutter,[55] M. Cooke,[47] W.E. Cooper,[47] M. Corcoran,[78] F. Couderc,[18] M.-C. Cousinou,[15] A. Croc,[18] D. Cutts,[75] M. Ćwiok,[30] A. Das,[44] G. Davies,[42] K. De,[76] S.J. de Jong,[34] E. De La Cruz-Burelo,[32] F. Déliot,[18] M. Demarteau,[47] R. Demina,[69] D. Denisov,[47] S.P. Denisov,[38] S. Desai,[47] K. DeVaughan,[64] H.T. Diehl,[47] M. Diesburg,[47] A. Dominguez,[64] T. Dorland,[80] A. Dubey,[28] L.V. Dudko,[37] D. Duggan,[65] A. Duperrin,[15] S. Dutt,[27] A. Dyshkant,[49] M. Eads,[64] D. Edmunds,[62] J. Ellison,[45] V.D. Elvira,[47] Y. Enari,[17] S. Eno,[58] H. Evans,[51] A. Evdokimov,[71] V.N. Evdokimov,[38] G. Facini,[60] A.V. Ferapontov,[75] T. Ferbel,[58,69] F. Fiedler,[24] F. Filthaut,[34] W. Fisher,[62] H.E. Fisk,[47] M. Fortner,[49] H. Fox,[41] S. Fuess,[47] T. Gadfort,[71] A. Garcia-Bellido,[69] V. Gavrilov,[36] P. Gay,[13] W. Geist,[19] W. Geng,[15,62] D. Gerbaudo,[66] C.E. Gerber,[48] Y. Gershtein,[65] D. Gillberg,[6] G. Ginther,[47,69] G. Golovanov,[35] A. Goussiou,[80] P.D. Grannis,[70] S. Greder,[19] H. Greenlee,[47] Z.D. Greenwood,[57] E.M. Gregores,[4] G. Grenier,[20] Ph. Gris,[13] J.-F. Grivaz,[16] A. Grohsjean,[18] S. Grünendahl,[47] M.W. Grünewald,[30] F. Guo,[70] J. Guo,[70] G. Gutierrez,[47] P. Gutierrez,[73] A. Haas[c],[68] P. Haefner,[25] S. Hagopian,[46] J. Haley,[60] L. Han,[7] K. Harder,[43] A. Harel,[69] J.M. Hauptman,[54] J. Hays,[42] T. Hebbeker,[21] D. Hedin,[49] A.P. Heinson,[45] U. Heintz,[75] C. Hensel,[23] I. Heredia-De La Cruz,[32] K. Herner,[61] G. Hesketh,[60] M.D. Hildreth,[53] R. Hirosky,[79] T. Hoang,[46] J.D. Hobbs,[70] B. Hoeneisen,[12] M. Hohlfeld,[24] S. Hossain,[73] Y. Hu,[70] Z. Hubacek,[10] N. Huske,[17] V. Hynek,[10] I. Iashvili,[67] R. Illingworth,[47] A.S. Ito,[47] S. Jabeen,[75] M. Jaffré,[16] S. Jain,[67] D. Jamin,[15] R. Jesik,[42] K. Johns,[44] M. Johnson,[47] D. Johnston,[64] A. Jonckheere,[47] P. Jonsson,[42] J. Joshi,[27] A. Juste[d],[47] K. Kaadze,[56] E. Kajfasz,[15] D. Karmanov,[37] P.A. Kasper,[47] I. Katsanos,[64] R. Kehoe,[77] S. Kermiche,[15] N. Khalatyan,[47] A. Khanov,[74] A. Kharchilava,[67] Y.N. Kharzheev,[35] D. Khatidze,[75] M.H. Kirby,[50] M. Kirsch,[21] J.M. Kohli,[27] A.V. Kozelov,[38] J. Kraus,[62] A. Kumar,[67] A. Kupco,[11] T. Kurča,[20] V.A. Kuzmin,[37] J. Kvita,[9] S. Lammers,[51] G. Landsberg,[75] P. Lebrun,[20] H.S. Lee,[31] W.M. Lee,[47] J. Lellouch,[17] L. Li,[45] Q.Z. Li,[47] S.M. Lietti,[5] J.K. Lim,[31] D. Lincoln,[47] J. Linnemann,[62] V.V. Lipaev,[38] R. Lipton,[47] Y. Liu,[7] Z. Liu,[6] A. Lobodenko,[39] M. Lokajicek,[11] P. Love,[41] H.J. Lubatti,[80] R. Luna-Garcia[e],[32] A.L. Lyon,[47] A.K.A. Maciel,[2] D. Mackin,[78] R. Madar,[18] R. Magaña-Villalba,[32] S. Malik,[64] V.L. Malyshev,[35] Y. Maravin,[56] J. Martínez-Ortega,[32] R. McCarthy,[70] C.L. McGivern,[55] M.M. Meijer,[34] A. Melnitchouk,[63] D. Menezes,[49] P.G. Mercadante,[4] M. Merkin,[37] A. Meyer,[21] J. Meyer,[23] N.K. Mondal,[29] T. Moulik,[55] G.S. Muanza,[15] M. Mulhearn,[79] E. Nagy,[15] M. Naimuddin,[28] M. Narain,[75] R. Nayyar,[28] H.A. Neal,[61] J.P. Negret,[8] P. Neustroev,[39] H. Nilsen,[22] S.F. Novaes,[5] T. Nunnemann,[25] G. Obrant,[39] D. Onoprienko,[56] J. Orduna,[32] N. Osman,[42] J. Osta,[53] G.J. Otero y Garzón,[1] M. Owen,[43] M. Padilla,[45] M. Pangilinan,[75] N. Parashar,[52] V. Parihar,[75] S.K. Park,[31] J. Parsons,[68] R. Partridge[c],[75] N. Parua,[51] A. Patwa,[71] B. Penning,[47] M. Perfilov,[37] K. Peters,[43] Y. Peters,[43] G. Petrillo,[69] P. Pétroff,[16] R. Piegaia,[1] J. Piper,[62] M.-A. Pleier,[71] P.L.M. Podesta-Lerma[f],[32] V.M. Podstavkov,[47] M.-E. Pol,[2] P. Polozov,[36] A.V. Popov,[38] M. Prewitt,[78] D. Price,[51] S. Protopopescu,[71] J. Qian,[61] A. Quadt,[23] B. Quinn,[63] M.S. Rangel,[16] K. Ranjan,[28] P.N. Ratoff,[41] I. Razumov,[38] P. Renkel,[77] P. Rich,[43] M. Rijssenbeek,[70] I. Ripp-Baudot,[19] F. Rizatdinova,[74] M. Rominsky,[47] C. Royon,[18]

P. Rubinov,[47] R. Ruchti,[53] G. Safronov,[36] G. Sajot,[14] A. Sánchez-Hernández,[32] M.P. Sanders,[25] B. Sanghi,[47] A.S. Santos,[5] G. Savage,[47] L. Sawyer,[57] T. Scanlon,[42] D. Schaile,[25] R.D. Schamberger,[70] Y. Scheglov,[39] H. Schellman,[50] T. Schliephake,[26] S. Schlobohm,[80] C. Schwanenberger,[43] R. Schwienhorst,[62] J. Sekaric,[55] H. Severini,[73] E. Shabalina,[23] V. Shary,[18] A.A. Shchukin,[38] R.K. Shivpuri,[28] V. Simak,[10] V. Sirotenko,[47] P. Skubic,[73] P. Slattery,[69] D. Smirnov,[53] G.R. Snow,[64] J. Snow,[72] S. Snyder,[71] S. Söldner-Rembold,[43] L. Sonnenschein,[21] A. Sopczak,[41] M. Sosebee,[76] K. Soustruznik,[9] B. Spurlock,[76] J. Stark,[14] V. Stolin,[36] D.A. Stoyanova,[38] E. Strauss,[70] M. Strauss,[73] R. Ströhmer,[25] D. Strom,[48] L. Stutte,[47] P. Svoisky,[34] M. Takahashi,[43] A. Tanasijczuk,[1] W. Taylor,[6] B. Tiller,[25] M. Titov,[18] V.V. Tokmenin,[35] D. Tsybychev,[70] B. Tuchming,[18] C. Tully,[66] P.M. Tuts,[68] R. Unalan,[62] L. Uvarov,[39] S. Uvarov,[39] S. Uzunyan,[49] R. Van Kooten,[51] W.M. van Leeuwen,[33] N. Varelas,[48] E.W. Varnes,[44] I.A. Vasilyev,[38] P. Verdier,[20] L.S. Vertogradov,[35] M. Verzocchi,[47] M. Vesterinen,[43] D. Vilanova,[18] P. Vint,[42] P. Vokac,[10] H.D. Wahl,[46] M.H.L.S. Wang,[69] J. Warchol,[53] G. Watts,[80] M. Wayne,[53] G. Weber,[24] M. Weber[g],[47] M. Wetstein,[58] A. White,[76] D. Wicke,[24] M.R.J. Williams,[41] G.W. Wilson,[55] S.J. Wimpenny,[45] M. Wobisch,[57] D.R. Wood,[60] T.R. Wyatt,[43] Y. Xie,[47] C. Xu,[61] S. Yacoob,[50] R. Yamada,[47] W.-C. Yang,[43] T. Yasuda,[47] Y.A. Yatsunenko,[35] Z. Ye,[47] H. Yin,[7] K. Yip,[71] H.D. Yoo,[75] S.W. Youn,[47] J. Yu,[76] S. Zelitch,[79] T. Zhao,[80] B. Zhou,[61] J. Zhu,[70] M. Zielinski,[69] D. Zieminska,[51] and L. Zivkovic[68]

(The D0 Collaboration*)

[1] *Universidad de Buenos Aires, Buenos Aires, Argentina*
[2] *LAFEX, Centro Brasileiro de Pesquisas Físicas, Rio de Janeiro, Brazil*
[3] *Universidade do Estado do Rio de Janeiro, Rio de Janeiro, Brazil*
[4] *Universidade Federal do ABC, Santo André, Brazil*
[5] *Instituto de Física Teórica, Universidade Estadual Paulista, São Paulo, Brazil*
[6] *Simon Fraser University, Vancouver, British Columbia, and York University, Toronto, Ontario, Canada*
[7] *University of Science and Technology of China, Hefei, People's Republic of China*
[8] *Universidad de los Andes, Bogotá, Colombia*
[9] *Charles University, Faculty of Mathematics and Physics, Center for Particle Physics, Prague, Czech Republic*
[10] *Czech Technical University in Prague, Prague, Czech Republic*
[11] *Center for Particle Physics, Institute of Physics, Academy of Sciences of the Czech Republic, Prague, Czech Republic*
[12] *Universidad San Francisco de Quito, Quito, Ecuador*
[13] *LPC, Université Blaise Pascal, CNRS/IN2P3, Clermont, France*
[14] *LPSC, Université Joseph Fourier Grenoble 1, CNRS/IN2P3, Institut National Polytechnique de Grenoble, Grenoble, France*
[15] *CPPM, Aix-Marseille Université, CNRS/IN2P3, Marseille, France*
[16] *LAL, Université Paris-Sud, CNRS/IN2P3, Orsay, France*
[17] *LPNHE, Universités Paris VI and VII, CNRS/IN2P3, Paris, France*
[18] *CEA, Irfu, SPP, Saclay, France*
[19] *IPHC, Université de Strasbourg, CNRS/IN2P3, Strasbourg, France*
[20] *IPNL, Université Lyon 1, CNRS/IN2P3, Villeurbanne, France and Université de Lyon, Lyon, France*
[21] *III. Physikalisches Institut A, RWTH Aachen University, Aachen, Germany*
[22] *Physikalisches Institut, Universität Freiburg, Freiburg, Germany*
[23] *II. Physikalisches Institut, Georg-August-Universität Göttingen, Göttingen, Germany*
[24] *Institut für Physik, Universität Mainz, Mainz, Germany*
[25] *Ludwig-Maximilians-Universität München, München, Germany*
[26] *Fachbereich Physik, Bergische Universität Wuppertal, Wuppertal, Germany*
[27] *Panjab University, Chandigarh, India*
[28] *Delhi University, Delhi, India*
[29] *Tata Institute of Fundamental Research, Mumbai, India*
[30] *University College Dublin, Dublin, Ireland*
[31] *Korea Detector Laboratory, Korea University, Seoul, Korea*
[32] *CINVESTAV, Mexico City, Mexico*
[33] *FOM-Institute NIKHEF and University of Amsterdam/NIKHEF, Amsterdam, The Netherlands*
[34] *Radboud University Nijmegen/NIKHEF, Nijmegen, The Netherlands*
[35] *Joint Institute for Nuclear Research, Dubna, Russia*
[36] *Institute for Theoretical and Experimental Physics, Moscow, Russia*
[37] *Moscow State University, Moscow, Russia*
[38] *Institute for High Energy Physics, Protvino, Russia*
[39] *Petersburg Nuclear Physics Institute, St. Petersburg, Russia*
[40] *Stockholm University, Stockholm and Uppsala University, Uppsala, Sweden*
[41] *Lancaster University, Lancaster LA1 4YB, United Kingdom*

[42]Imperial College London, London SW7 2AZ, United Kingdom
[43]The University of Manchester, Manchester M13 9PL, United Kingdom
[44]University of Arizona, Tucson, Arizona 85721, USA
[45]University of California Riverside, Riverside, California 92521, USA
[46]Florida State University, Tallahassee, Florida 32306, USA
[47]Fermi National Accelerator Laboratory, Batavia, Illinois 60510, USA
[48]University of Illinois at Chicago, Chicago, Illinois 60607, USA
[49]Northern Illinois University, DeKalb, Illinois 60115, USA
[50]Northwestern University, Evanston, Illinois 60208, USA
[51]Indiana University, Bloomington, Indiana 47405, USA
[52]Purdue University Calumet, Hammond, Indiana 46323, USA
[53]University of Notre Dame, Notre Dame, Indiana 46556, USA
[54]Iowa State University, Ames, Iowa 50011, USA
[55]University of Kansas, Lawrence, Kansas 66045, USA
[56]Kansas State University, Manhattan, Kansas 66506, USA
[57]Louisiana Tech University, Ruston, Louisiana 71272, USA
[58]University of Maryland, College Park, Maryland 20742, USA
[59]Boston University, Boston, Massachusetts 02215, USA
[60]Northeastern University, Boston, Massachusetts 02115, USA
[61]University of Michigan, Ann Arbor, Michigan 48109, USA
[62]Michigan State University, East Lansing, Michigan 48824, USA
[63]University of Mississippi, University, Mississippi 38677, USA
[64]University of Nebraska, Lincoln, Nebraska 68588, USA
[65]Rutgers University, Piscataway, New Jersey 08855, USA
[66]Princeton University, Princeton, New Jersey 08544, USA
[67]State University of New York, Buffalo, New York 14260, USA
[68]Columbia University, New York, New York 10027, USA
[69]University of Rochester, Rochester, New York 14627, USA
[70]State University of New York, Stony Brook, New York 11794, USA
[71]Brookhaven National Laboratory, Upton, New York 11973, USA
[72]Langston University, Langston, Oklahoma 73050, USA
[73]University of Oklahoma, Norman, Oklahoma 73019, USA
[74]Oklahoma State University, Stillwater, Oklahoma 74078, USA
[75]Brown University, Providence, Rhode Island 02912, USA
[76]University of Texas, Arlington, Texas 76019, USA
[77]Southern Methodist University, Dallas, Texas 75275, USA
[78]Rice University, Houston, Texas 77005, USA
[79]University of Virginia, Charlottesville, Virginia 22901, USA
[80]University of Washington, Seattle, Washington 98195, USA

(Dated: June 17, 2010)

We present a search for flavor changing neutral currents via quark-gluon couplings in a sample of single top quark final states corresponding to 2.3 fb^{-1} of integrated luminosity collected with the D0 detector at the Fermilab Tevatron Collider. We select events containing a single top quark candidates with an additional jet, and obtain separation between signal and background using Bayesian neural networks. We find consistency between background expectation and observed data, and set limits on flavor changing neutral current gluon couplings of the top quark to up quarks (tgu) and charm quarks (tgc). The cross section limits at the 95% C.L. are $\sigma_{tgu} < 0.20$ pb and $\sigma_{tgc} < 0.27$ pb. These correspond to limits on the top quark decay branching fractions of $\mathcal{B}(t \to gu) < 2.0 \times 10^{-4}$ and $\mathcal{B}(t \to gc) < 3.9 \times 10^{-3}$.

PACS numbers: 14.65.Ha, 12.15.Ji, 13.85.Qk

The observation of electroweak production of single top quarks was reported in 2009 [1, 2]. Those measurements, as well as the evidence for t-channel single top quark production [3], focus on standard model (SM) production of single top quarks. The single top quark final state is sensitive to several models of physics beyond the SM [4], in particular those in which flavor changing neutral current (FCNC) couplings between a gluon, a top quark, and up or charm quarks may be large. Examples include models with multiple Higgs doublets

*with visitors from [a]Augustana College, Sioux Falls, SD, USA, [b]The University of Liverpool, Liverpool, UK, [c]SLAC, Menlo Park, CA, USA, [d]ICREA/IFAE, Barcelona, Spain, [e]Centro de Investigacion en Computacion - IPN, Mexico City, Mexico, [f]ECFM, Universidad Autonoma de Sinaloa, Culiacán, Mexico, and [g]Universität Bern, Bern, Switzerland.

such as supersymmetry [5–7], those with new dynamical interactions of the top quark [8–10], or models in which the top quark is a composite object [11] or has a soliton structure [12, 13]. In principle, such interactions can also be produced through SM higher-order radiative corrections; however, their effects are too small to be observed [5]. Stringent limits exist for FCNC top quark couplings to photons and Z bosons from studies of production and decay of top quarks [14–17]. The first limits on gluon FCNC couplings to the top quark were obtained in a D0 analysis based on 0.23 fb^{-1} of integrated luminosity [18]. The CDF Collaboration searched for FCNC production of single top quarks, without extra jets, through gluon-quark interactions [19, 20], using a dataset corresponding to 2.2 fb^{-1} of integrated luminosity [21]. The limits on the FCNC couplings are $\kappa_{tgu}/\Lambda < 0.018$ TeV^{-1} and $\kappa_{tgc}/\Lambda < 0.069$ TeV^{-1}, where Λ is the scale of the new interactions which generate these couplings (of order 1 TeV).

The FCNC coupling of a gluon to a top quark and a light quark results in either s-channel production and decay [Fig. 1 (a) and (d)] or in t-channel exchange [Fig. 1 (b) and (c)] of a virtual particle. The largest contribution to the production cross section (83% for tgu and 66% for tgc) is from the diagram in Fig. 1 (a). The final state in each case contains a top quark and a light quark or gluon, a topology similar to SM t-channel single top quark production. We do not consider the single top quark final state without extra jets that was explored by the CDF Collaboration [21] due to its different final state topology and significantly smaller signal event yield for a given coupling.

The FCNC couplings can be parametrized in a model-independent way, using an effective Lagrangian [22, 23] of the form:

$$\mathcal{L}_{\rm FCNC} = \frac{\kappa_{tgf}}{\Lambda} g_s \bar{f} \sigma^{\mu\nu} \frac{\lambda^a}{2} t G^a_{\mu\nu}, \qquad (1)$$

where $f = u$ or c, with u, c and t representing the quark fields; κ_{tgf} defines the strength of the tgu or tgc couplings; g_s and λ^a are the strong coupling constant and color matrices; $\sigma^{\mu\nu}$ and $G^a_{\mu\nu}$ are the Dirac tensor and the gauge field tensor of the gluon. The FCNC single top quark production cross section depends therefore quadratically on the factor κ_{tgf}/Λ. For a coupling of $\kappa_{tgf}/\Lambda = 0.015$ TeV^{-1}, the next-to leading order (NLO) cross sections at a top quark mass of 170 GeV are $\sigma^{\rm NLO}_{tgu} = 0.29$ pb and $\sigma^{\rm NLO}_{tgc} = 0.020$ pb [24]. The top quark decay branching fraction to a gluon and any quark also depends quadratically on the factor κ_{tgf}/Λ [25], but this branching fraction is negligible for coupling factors considered in this analysis [23].

We search for FCNC production of single top quarks in association with a quark or gluon, where the top quark decays to a W boson and a b quark, and the W boson subsequently decays to a lepton (electron or muon) and a neutrino. The main backgrounds to this final state are from W+jets production, including $W + c$-quarks and $W + b$-quarks, with smaller contributions from $t\bar{t}$, SM single top quarks ($tb + tqb$), as well as multijets, dibosons, and Z+jets production. We base the analysis on the dataset and event selection from the single top quark production observation Letter [1], using 2.3 fb^{-1} of integrated luminosity collected with the D0 detector [26] at the Fermilab Tevatron Collider.

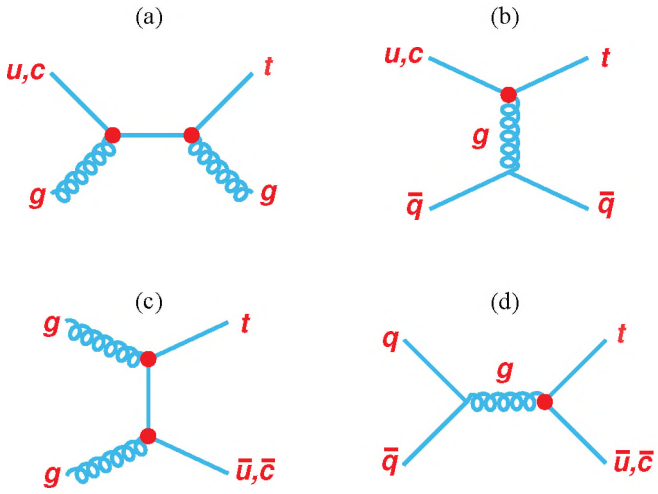

FIG. 1: Leading order Feynman diagrams for FCNC gluon coupling between an up or a charm quark and a top quark.(a) and (d) show two s-channel diagrams for the tg final state and the tq final state and (b) and (c) are two t-channel diagrams for the tq final state. The circles indicate the effective FCNC coupling, possible at either of the two vertices in (a) and (c), for which the amplitudes are properly summed.

The detector has a central tracking system, consisting of a silicon microstrip tracker and a central fiber tracker, both located within a 1.9 T superconducting solenoidal magnet, with designs optimized for tracking and vertexing at pseudorapidities $|\eta| < 3$ and $|\eta| < 2.5$, respectively [27–29]. A liquid-argon and uranium calorimeter has a central section covering pseudorapidities $|\eta|$ up to ≈ 1.1, and two end calorimeters that extend coverage to $|\eta| \approx 4.2$, with all three housed in separate cryostats [30]. An outer muon system, at $|\eta| < 2$, consists of a layer of tracking detectors and scintillation trigger counters in front of 1.8 T toroids, followed by two similar layers after the toroids [31].

We select events containing a lepton, missing transverse energy ($\not\!\!E_T$), and two to four jets with transverse momentum $p_T > 15$ GeV and $|\eta| < 3.4$ (allowing for jets from gluon radiation), with the leading (highest p_T) jet additionally satisfying $p_T > 25$ GeV [32]. We require $20 < \not\!\!E_T < 200$ GeV for events with two jets and $25 < \not\!\!E_T < 200$ GeV for events with three or four jets. Events must contain only one isolated electron with

$p_T > 15$ GeV and $|\eta| < 1.1$ ($p_T > 20$ GeV for three- or four-jet events), or one isolated muon with $p_T > 15$ GeV and $|\eta| < 2.0$. The multijets background, where a jet is misidentified as an isolated lepton, is kept to approximately 5% of the total background by requiring the scalar sum of all transverse energies, $H_T(\text{lepton}, \not\!\!E_T, \text{alljets})$, to be greater than 110 to 160 GeV, depending on the lepton flavor and jet multiplicity, and by requiring that the $\not\!\!E_T$ is not colinear with the axes of the lepton or the leading jet in the transverse plane. To enhance the fraction of top quark events, one of the jets is required to be identified as originating from b quark fragmentation through a neural network (NN) b-tagging algorithm [33]. To partially reject background from $W + b\bar{b}$, $t\bar{t}$, and SM single top quark events, each event is required to contain only one b-tagged jet (vetoing double-tagged events), in contrast to SM single top quark analyses where double-tagged events are also considered.

We model the FCNC signals and SM single top quark background with the SingleTop Monte Carlo (MC) generator [34], using CTEQ6M parton distribution functions [35, 36]. The ALPGEN leading-order MC event generator [37], interfaced to PYTHIA for showering and hadronization [38], is used to model $t\bar{t}$, W+jets, and Z+jets background, while PYTHIA is used to model diboson (WW, WZ and ZZ) production. We set the mass of the top quark to 170 GeV, and use the CTEQ6L1 parton distribution functions [35, 36]. We use GEANT [39] to simulate the response of the D0 detector to MC events. To model the effects of multiple interactions and detector noise, data from random $p\bar{p}$ crossings are overlaid on MC events. The SM single top quark, $t\bar{t}$, diboson and Z+jets backgrounds are normalized to their predicted cross sections [40–42]. The W+jets background normalization and jet angular distributions are obtained from data samples without b-tagging requirements, and its flavor composition is determined from data samples with different numbers of b-tagged jets. We model the background from multijets production using data containing lepton candidates that fail one of the lepton identification requirements, but otherwise resemble the signal events. In the muon channel, where a secondary muon in a jet is misidentified as an isolated muon, this is accomplished by reversing the tight isolation criterion, whereas in the electron channel, where a jet is misidentified as an electron, we reverse the tight electron identification criteria [43, 44].

We select a total of 3735 lepton+jets data events with only one b-tagged jet. The sample composition is given in Table I.

We further improve the sensitivity to FCNC through an application of Bayesian neural networks (BNN) [44–46], with settings identical to those detailed in Ref. [1]. A BNN is an average over many individual neural networks [47] (100 networks are used in this analysis), where the parameters for each network are sampled from the Bayesian posterior density distribution of the entire network parameter space.

TABLE I: Event yields with uncertainty for each jet multiplicity for the electron and muon channels combined. The FCNC signals are each normalized to their observed cross section upper limits. The uncertainty on the total background includes correlations amongst sources.

Source	2 jets	3 jets	4 jets
FCNC signal			
tgu	34 ± 4	16 ± 3	5 ± 1
tgc	54 ± 7	23 ± 4	7 ± 2
Background			
W+jets	1660 ± 146	560 ± 54	154 ± 15
Z+jets and dibosons	204 ± 34	72 ± 14	22 ± 6
SM single top	112 ± 15	46 ± 7	14 ± 3
$t\bar{t}$	152 ± 24	277 ± 42	278 ± 41
Multijets	184 ± 47	66 ± 15	27 ± 5
Total background	2312 ± 170	1021 ± 84	495 ± 53
Data	2277	958	500

We use 54 discriminating variables, a subset of those used in each channel of the single top quark observation analysis [1] plus those from the previous FCNC analysis [18]. The set of variables comprises individual object and event kinematics, top quark reconstruction, jet width, and angular correlations. Figure 2 compares the observed data to the background model for six illustrative discriminating variables. Object kinematics, such as the leading jet p_T, and event kinematics, such as the invariant mass of the all-jets system, help separate the FCNC signals from the W+jets background. Jet reconstruction variables, such as the width in η of the second leading jet, provide additional separation of light quark jets and heavy flavor jets. Angular variables such as the cosine between lepton and leading jet, or the ϕ difference between lepton and $\not\!\!E_T$, separate FCNC interactions from all backgrounds. Reconstruction of the top quark by combining the W boson with one of the jets discriminates against the W+jets background. The top quark mass reconstructed with the leading jet separates FCNC signal events (where the leading jet typically comes from the top quark decay) from all backgrounds including $t\bar{t}$ (where the leading jet comes from one of the two top quark decays).

Since their kinematics are similar, the two FCNC processes are combined into a single signal for training the BNN, each normalized to the same coupling. Separate BNNs are trained for each choice of lepton flavor (electron or muon), jet multiplicity (2, 3, or 4), and data-taking period, twelve in total. Each utilizes 23 or 24 variables, selected from the list of 54, to provide the highest sensitivity for each analysis channel. Figure 3 shows the comparison between background and data for all twelve BNN discriminants combined. A Kolmogorov-Smirnov test comparing the observed data to the background sum in Figs. 3(a) and 3(b) gives values of 0.38 and 1.0, respectively, demonstrating that the

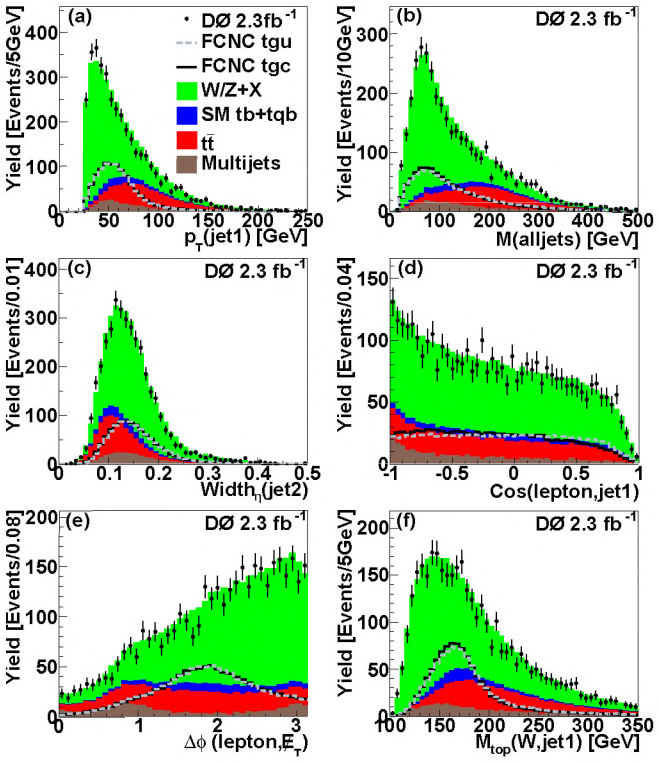

FIG. 2: Comparison of the background model to data for several discriminating variables summed over all analysis channels: (a) p_T of the leading jet, (b) invariant mass of the system of all jets, (c) width in pseudorapidity of the second leading jet, (d) cosine of the angle between the leading jet and the lepton, (e) ϕ separation between the lepton and $\not\!\!E_T$, and (f) top quark mass reconstructed from the reconstructed W boson and the leading jet. The FCNC signals are normalized to cross sections of 5 pb to visualize them clearly, and $W/Z + X$ includes W+jets and smaller backgrounds from Z+jets and dibosons.

background model reproduces the data well.

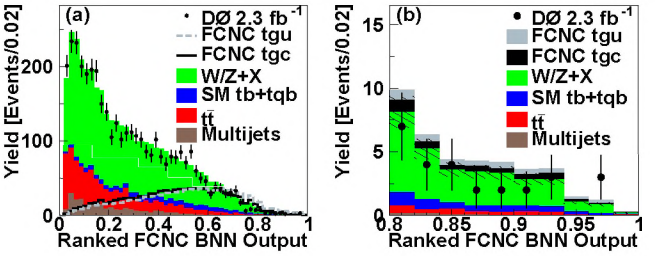

FIG. 3: Comparison of the background model to data for the FCNC discriminant summed over all analysis channels, (a) for the whole discriminant range and (b) only the high discriminant region, where the hatched region gives the uncertainty on the background sum. The bins have been ordered by their signal to background ratio and the FCNC signals are each normalized to a cross section of 5 pb in (a) and to their observed limits in (b). $W/Z+X$ includes W+jets and smaller backgrounds from Z+jets and dibosons.

Systematic uncertainties on the modeling of signal and background are described in Ref. [44], with main uncertainties being from corrections to the jet energy scale and the b-tag modeling, with smaller contributions arising from MC statistics, corrections for jet-flavor composition in W+jets events, and from the normalization of W+jets, multijets, and $t\bar{t}$ production. The total uncertainty on the background is (8–16)%, depending on the analysis channel. For jet energy scale, b-tag modeling and W+jets modeling, we vary not only the normalization but also consider effects on the shape of the final discriminant. When setting limits on the FCNC couplings, an additional signal cross section uncertainty of 8.8% from the NLO calculation is included [24].

Since the data are consistent with the background expectation, we set upper limits on the FCNC cross sections and couplings using a Bayesian approach [48]. Following the analysis strategy of our previous work [18], we form a two-dimensional Bayesian posterior density for the cross sections and for the square of the FCNC couplings, using the BNN distributions for data, background, and signals. Systematic uncertainties are taken into account with Gaussian priors, including correlations among bins and signal and background sources. We choose priors that are flat and non-negative in the FCNC couplings squared and hence in the FCNC cross sections. The posterior density as a function of the FCNC cross sections σ_{tgu} and σ_{tgc} is shown in Fig. 4(a). We similarly form a two-dimensional Bayesian posterior density as a function of the $(\kappa_{tgf}/\Lambda)^2$, as shown in Fig. 4(b), adding systematic uncertainties to the FCNC cross sections.

One-dimensional posterior densities as a function of σ_{tgu} and σ_{tgc} are derived from the general two-dimensional posterior, by integrating over the σ_{tgc} or σ_{tgu} axes, respectively. One-dimensional posteriors are similarly derived as a function of $(\kappa_{tgu}/\Lambda)^2$ and $(\kappa_{tgc}/\Lambda)^2$ and are shown in Fig. 5. This procedure keeps the measurement free of theoretical assumptions concerning the relationship between the two FCNC cross sections and couplings. For each quantity, we also compute expected limits by replacing the count in data in each bin by the background sum. The expected posterior densities for $(\kappa_{tgu}/\Lambda)^2$ and $(\kappa_{tgc}/\Lambda)^2$ are also shown in Fig. 5, together with the 95% C.L. limits. The observed limits are below the expected limits, consistent with Fig. 3(b), which shows that the data count is below the background expectation for several bins in the high BNN output region. Since the FCNC decay branching fraction is proportional to the square of the coupling, the limits on the couplings can be translated into decay branching fraction limits based on the NLO calculation [25]. The limits on cross sections, couplings and branching fractions are summarized in Table II.

In summary, we have presented a search for FCNC interactions in the gluon coupling of top quarks to

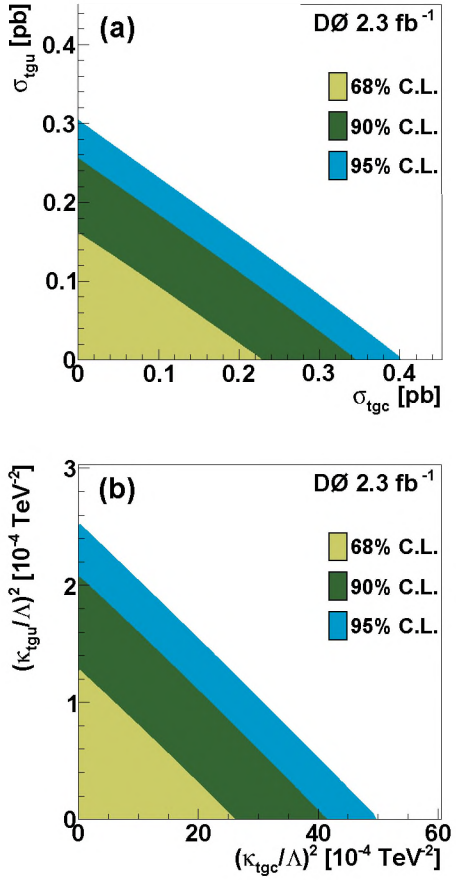

FIG. 4: Bayesian posterior probability as a function of (a) the σ_{tgu} and σ_{tgc} cross sections and (b) the squares of the couplings.

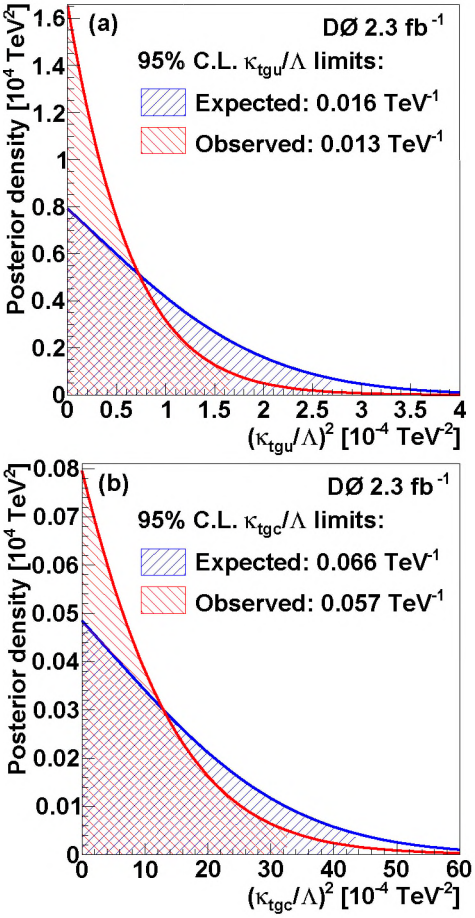

FIG. 5: One-dimensional Bayesian posterior probability as a function of (a) $(\kappa_{tgu}/\Lambda)^2$ and (b) $(\kappa_{tgc}/\Lambda)^2$.

TABLE II: Observed 95% C.L. upper one-dimensional limits on the FCNC cross sections, couplings, and branching fractions.

	tgu	tgc
Cross section	0.20 pb	0.27 pb
κ_{tgf}/Λ	0.013 TeV^{-1}	0.057 TeV^{-1}
$\mathcal{B}(t \to fg)$	2.0×10^{-4}	3.9×10^{-3}

up quarks or charm quarks. Using a sample of 2.3 fb^{-1} of integrated luminosity recorded by the D0 experiment at the Tevatron Collider at Fermilab, we set limits on the couplings of $\kappa_{tgu}/\Lambda < 0.013$ TeV^{-1} and $\kappa_{tgc}/\Lambda < 0.057$ TeV^{-1}, without making assumptions about the tgc and tgu couplings, respectively. The corresponding limits on top quark decay branching fractions are $\mathcal{B}(t \to gu) < 2.0 \times 10^{-4}$ and $\mathcal{B}(t \to gc) < 3.9 \times 10^{-3}$. These branching fraction limits are the most stringent and improve on the previous best limits by factors of two for $\mathcal{B}(t \to gu)$ and 1.5 for $\mathcal{B}(t \to gc)$ [21]. They improve on D0's previous result by a factor eight as a result of a larger data set and significant improvements in analysis [18].

We thank the staffs at Fermilab and collaborating institutions, and acknowledge support from the DOE and NSF (USA); CEA and CNRS/IN2P3 (France); FASI, Rosatom and RFBR (Russia); CNPq, FAPERJ, FAPESP and FUNDUNESP (Brazil); DAE and DST (India); Colciencias (Colombia); CONACyT (Mexico); KRF and KOSEF (Korea); CONICET and UBACyT (Argentina); FOM (The Netherlands); STFC and the Royal Society (United Kingdom); MSMT and GACR (Czech Republic); CRC Program and NSERC (Canada); BMBF and DFG (Germany); SFI (Ireland); The Swedish Research Council (Sweden); and CAS and CNSF (China).

[1] V. M. Abazov *et al.* (D0 Collaboration), Phys. Rev. Lett. **103**, 092001 (2009).
[2] T. Aaltonen *et al.* (CDF Collaboration), Phys. Rev. Lett. **103**, 092002 (2009).
[3] V. M. Abazov *et al.* (D0 Collaboration), Phys. Lett. B **682**, 363 (2010).
[4] T. Tait and C.-P. Yuan, Phys. Rev. D **63**, 014018 (2001).
[5] G. Eilam, J. L. Hewett, and A. Soni, Phys. Rev. D **44**, 1473 (1991).

[6] D. Atwood, L. Reina and, A. Soni, Phys. Rev. D **53**, 1199 (1996).

[7] J. M. Yang, B.-L. Young, and X. Zhang, Phys. Rev. D **58**, 055001 (1998).

[8] C. T. Hill, Phys. Lett. B **266**, 419 (1991); *ibid.* **345**, 483 (1995).

[9] B. Holdom, Phys. Lett. B **339**, 114 (1994); *ibid.* **351**, 279 (1995).

[10] H. J. Zhang, Phys. Rev. D **77**, 057501 (2008).

[11] H. Georgi, L. Kaplan, D. Morin, and A. Schenk, Phys. Rev. D **51**, 3888 (1995).

[12] X. Zhang, Phys. Rev. D **51**, 5309 (1995).

[13] J. Berger, A. Blotz, H. C. Kim, and K. Goeke, Phys. Rev. D **54**, 3598 (1996).

[14] F. Abe *et al.* (CDF Collaboration), Phys. Rev. Lett. **80**, 2525 (1998).

[15] T. Aaltonen *et al.* (CDF Collaboration), Phys. Rev. Lett. **101**, 192002 (2008).

[16] P. Achard *et al.* (L3 Collaboration), Phys. Lett. B **549**, 290 (2002).

[17] S. Chekanov *et al.* (ZEUS Collaboration), Phys. Lett. B **559**, 153 (2004).

[18] V. M. Abazov *et al.* (D0 Collaboration), Phys. Rev. Lett. **99**, 191802 (2007).

[19] L. L. Yang, C. S. Li, Y. Gao, and J. J. Liu, Phys. Rev. D **73**, 074017 (2006).

[20] J. Gao, C. S. Li, J. J. Zhang, and H. X. Zhu, Phys. Rev. D **80**, 114017 (2009).

[21] T. Aaltonen *et al.* (CDF Collaboration), Phys. Rev. Lett. **102**, 151801 (2009).

[22] T. Han, K. Whisnant, B.-L. Young, and X. Zhang, Phys. Lett. B **385**, 311 (1996).

[23] M. Hosch, K. Whisnant, and B.-L. Young, Phys. Rev. D **56**, 5725 (1997).

[24] J. J. Liu, C. S. Li, L. L. Yang, and L. G. Jin, Phys. Rev. D **72**, 074018 (2005).

[25] J. J. Zhang *et al.*, Phys. Rev. Lett. **102**, 072001 (2009).

[26] V. M. Abazov *et al.* (D0 Collaboration), Nucl. Instrum. Methods Phys. Res. A **565**, 463 (2006).

[27] S. N. Ahmed *et al.*, arXiv:1005.0801 [physics.ins-det] (2010), submitted for publication in Nucl. Instrum. Methods Phys. Res. A.

[28] R. Angstadt *et al.*, arXiv:0911.2522 [physics.ins-det] (2009), accepted for publication in Nucl. Instrum. Methods Phys. Res. A.

[29] Pseudorapidity is defined as $\eta = -\ln[\tan(\theta/2)]$, where θ is the polar angle with respect to the beam axis and the origin at the interaction vertex.

[30] S. Abachi *et al.* (D0 Collaboration), Nucl. Instrum. Methods Phys. Res. A **338**, 185 (1994).

[31] V. M. Abazov *et al.*, Nucl. Instrum. Methods Phys. Res. A **552**, 372 (2005).

[32] Jets are defined using the iterative seed-based cone algorithm with radius $\mathcal{R} = \sqrt{(\Delta\phi)^2 + (\Delta\eta)^2} = 0.5$, including midpoints as described on pp. 47–77 in G.C. Blazey *et al.*, in *Proceedings of the Workshop on QCD and Weak Boson Physics in Run II*, edited by U. Baur, R.K. Ellis, and D. Zeppenfeld, FERMILAB-PUB-00-297 (2000).

[33] V. M. Abazov *et al.* (D0 Collaboration), Nucl. Instrum. Methods Phys. Res. A. **620**, 490 (2010).

[34] E. E. Boos *et al.*, Phys. Atom. Nucl. **69**, 1317 (2006); E. E. Boos *et al.* (CompHEP Collaboration), Nucl. Instrum. Methods Phys. Res. A **534**, 250 (2004). We use SingleTop version 4.2p1.

[35] J. Pumplin *et al.* (CTEQ Collaboration), JHEP **07** , 012 (2002).

[36] D. Stump *et al.* (CTEQ Collaboration), JHEP **10**, 046 (2003).

[37] M. L. Mangano *et al.*, JHEP **07**, 001 (2003). We use ALPGEN version 2.11.

[38] T. Sjöstrand, S. Mrenna, and P. Skands, JHEP **05**, 026. (2006). We use PYTHIA version 6.409.

[39] R. Brun and F. Carminati, CERN Program Library Long Writeup W5013, 1993 (unpublished). We use GEANT version 3.21.

[40] N. Kidonakis and R. Vogt, Phys. Rev. D **68**, 114014 (2003). At $m_t = 170$ GeV, $\sigma(p\bar{p} \to t\bar{t} + X) = 7.91$ pb.

[41] N. Kidonakis, Phys. Rev. D **74**, 114012 (2006). At $m_t =$ 170 GeV, $\sigma(p\bar{p} \to (tb + X,\ tqb + X)) = 3.46$ pb.

[42] J. M. Campbell and R. K. Ellis, Phys. Rev. D **65**, 113007 (2002). We use MCFM version 5.1.

[43] A. P. Heinson, Mod. Phys. Lett. A **25**, 309 (2010).

[44] V. M. Abazov *et al.* (D0 Collaboration), Phys. Rev. D **78**, 012005 (2008).

[45] R. M. Neal, *Bayesian Learning for Neural Networks* (Springer-Verlag, New York, 1996).

[46] A. Tanasijczuk, Ph.D. thesis, Universidad de Buenos Aires, FERMILAB-THESIS-2010-20 (2010).

[47] C. M. Bishop, *Neural Networks for Pattern Recognition* (Clarendon Press, Oxford, 1998).

[48] I. Bertram *et al.*, FERMILAB-TM-2104 (2000) (unpublished).